

# Active Flow Control on Laminar flow over a Backward facing step

**Aditya Mushyam\*, Josep M Bergada**

Fluid Mechanics Department  
 Technical University of Catalunya  
 Terrassa, Barcelona, Spain-08222

\*mushyam.aditya@gmail.com

**Abstract.** In the present study, two dimensional flow over a backward-facing step in laminar flow regime with application of active flow control (AFC) technique is analysed. The aim of the present work is to gauge the effectiveness of implementing AFC to reduce drag and study its effects on flow characteristics. In order to analyse the influence of AFC on the boundary layer and the downstream vortex shedding, two different kinds of AFC techniques have been used in this study namely zero net mass flow actuators and fluidic actuators. A parametric non dimensional analysis has been carried out by varying the frequency from 0.025 to 0.1 and jet amplitude from 0.05 and 1. Four different positions of the groove were simulated; groove was respectively located at 0.024a, 0.047a, 0.072a and 0.097a, measured upstream from the right side upper edge. Three different non dimensional groove widths 0.023a, 0.048a and 0.073a were also evaluated, where a is the step height. The idea behind this study was to determine an optimal configuration to reduce the drag on the step and to suppress the vortex dissipation in the wake of the step. It was observed that when using an AFC frequency  $\pm 10\%$  of the vortex shedding one, was causing the maximum drag reduction. When comparing the effects of zero net mass flow actuators with the fluidic actuators, it was observed that zero net mass flow actuators were more effective.

## Nomenclature:

a	Height of the inclined step	(m)
A	Amplitude of the AFC jet	
$C_D$	Drag coefficient	
$C_L$	Lift coefficient	
f	Frequency of AFC	
h	Height of the non-orthogonal physical domain	
l	Length of the non-orthogonal physical domain	
p	Non dimensional Pressure	
Re	Reynolds number	
t	Non-dimensional Time	
ul	Upstream Length of the physical domain	
u	Non-dimensional Velocity Y direction	
U	Free stream velocity in X direction at the inlet	(m/sec)
v	Non-dimensional Velocity Y direction	
w	Width of the groove	



x	Non-Dimensional Eulerian coordinates in horizontal direction
y	Non-Dimensional Eulerian coordinates in vertical direction
$\phi$	Additional default amplitude of the AFC jet

## 1. Introduction:

Among the previous research undertaken on AFC on backwards facing step, study carried out by Dahan et al [1] can be noted. They performed a 2D and 3D numerical study using Reynolds number,  $Re=280$  and  $1500$  respectively with both open and closed loop control. Two different locations of the zero net mass flow actuators were considered, namely near the separation border and close to the step foot. They observed that perturbing the flow with a frequency close to the shedding frequency, increased the turbulent kinetic energy in the near separation region and decreased the base pressure. Dejoan et al [2] numerically studied the effect of a 2D ZNMF actuator located just before the separation corner with a jet inclination of  $45^\circ$ , the same inclination also used by Dahan et al [1]. Marrot et al [3] used a loudspeaker located downstream of the step to activate the boundary layer, that maximum effect was observed when the loudspeaker frequency was equal to the boundary layer instability mode. At these conditions a small reduction of the recirculation length was obtained. The pre exited flow was controlled using two rows of synthetic jets located on the vertical side of the step. A similar method, consisting of two arrays of jets located on the vertical side of the step of which the upper row steadily absorbs and the lower row steadily injects, was analysed numerically in 2D by Creusé et al [4], in fact different AFC techniques including pulsating flow were evaluated. As in Dahan et al [1], and Marrot et al [3], open loop and closed loop control were studied. For open loop control, the optimum actuation frequency, as already found by many other researchers, coincided with the fundamental frequency, which was  $St_h = 0.14$ , the optimum amplitude being  $A=0.2$ , this was the same amplitude used by Dahan et al [1]. According to the work presented in Hassan [5], in laminar flow conditions, the shear layer has two instability modes defined by a Strouhal number,  $S_{r\theta} = f \theta / U$ , where  $\theta$  is the momentum thickness of the boundary layer on the step edge,  $f$  is the natural roll up frequency of the shear layer and  $U$  is the free stream velocity. The step mode based on the step height  $h$ , is defined by Strouhal number,  $S_{rh} = f h / U$ . He observed these values to be around  $S_{r\theta} = 0.012$  and  $S_{rh} = 0.185$  and these values match with the values obtained lately in Marrot et al [3],  $St_h = 0.14$  and Dejoan et al [2],  $St_h = 0.2$ . It was reported that a slight waviness of energy in the boundary layer results in a periodic vortex train, as defined by Vukasinovic et al [6]. The location, frequency, amplitude and of course the overall amount of energy of the AFC in each particular application is nowadays an interesting field of research.

## 2. Problem Statement

Figure 1 presents the physical domain of the inclined step. Flow over a Backward facing step with upstream length,  $ul=2a$  and downstream length  $dl=20a$ , was simulated at Reynolds number  $Re 500$ . No slip boundary condition was used at all solid boundaries. Flow was simulated in two dimensions and under laminar regime. The AFC groove was placed at four different locations, measured upstream of the upstream surface edge. Figure 1 also presents the boundary conditions used for the simulation. Structured grid has been generated using the stretching transformation proposed by Roberts [7], which refines the grid in the vicinity of the solid walls. Two different types of active flow control techniques were studied namely zero net mass flow and fluidic actuators and a brief explanation and formulation follows.

Zero-net mass flow control technique, (ZNMF):

In this technique, the flow is injected into the flow upstream of the step such that the net mass flow from the groove is zero, in a cycle. A sinusoidal form of wave equation was used to induce the flow control technique as presented in equation 1.

$$\begin{aligned} u &= 0 \\ v &= A U \sin(2 \pi f t) \end{aligned} \quad (1)$$

Where  $u$  is the horizontal  $x$ -component and  $v$  is the vertical  $y$ -component of jet velocity respectively,  $f$  is the frequency of the active flow control jet and  $t$  is the time.  $A$  is the amplitude of the jet with respect to free stream velocity  $U$ .

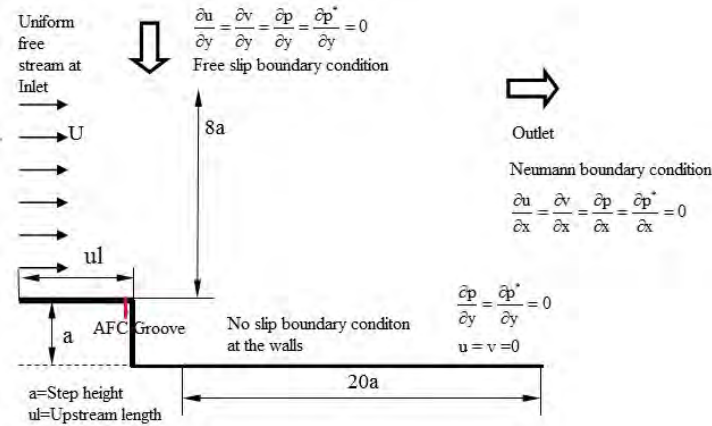


Figure 1: Physical Domain of the backwards facing Step

Fluidic Actuator flow control technique, (FA):

In fluidic actuators, the flow control is induced into the flow upstream of the step, in such a way that there is net outgoing mass flow from the groove. This the primary difference between (ZNMF) and (FA) techniques. This net outwards mass flow is applied by inducing a default constant amplitude  $\Phi$ , in addition to the sinusoidal wave equation used in zero net mass flow technique, as presented in equation 2. In the the present study for all the cases of FA, the amplitude  $\Phi$  was considered equal to the amplitude  $A$ .

$$\begin{aligned} u &= 0 \\ v &= \Phi + A U \sin(2 \pi f t) \end{aligned} \quad (2)$$

For both configurations (ZNMF) and (FA), the non-dimensional frequency was varied in a range from  $f = 0.025$  to  $0.1$  and the jet amplitude,  $A$  between  $0.05$  and  $1$ .

The effect of groove implementing AFC, was studied for four different positions of the groove at  $0.024a$ ,  $0.047a$ ,  $0.072a$  and  $0.097a$ , measured on the upstream surface edge of the step. Also three different non dimensional groove widths were considered,  $0.023a$ ,  $0.048a$  and  $0.073a$ , where  $a$ , is the step height. The main aim of this study is to determine an optimum configuration which results in the suppression or minimization of drag on the step.

## 2.1 Governing Equations:

Simulations have been done with non-dimensional form of Navier-Stokes equations. Flow was considered as isothermal. The height of the step,  $a$ , was taken as the characteristic length, upstream velocity  $U$  was used as characteristic velocity. The characteristic pressure was defined as  $\rho U^2$  and the characteristic time was defined as the characteristic length divided by the characteristic velocity  $a/U$ .

Reynolds number was defined as  $Re = \frac{\rho U a}{\mu}$ ; Fluid density  $\rho$  and viscosity  $\mu$ , were taken as constant.

## 2.2 Numerical Strategy and Boundary Conditions:

A second-order Adams Bashforth-Crank Nicholson scheme for temporal discretization was applied to Navier Stokes equations in finite volume formulation. The boundary conditions used in the simulation were depicted in figure 1. MAC (Marker and Cell) method with velocity and pressure coupling was applied using a predictor-corrector strategy. In the present study, the respective pressure correction factor in all the neighboring cells were also considered, notice that this is a further improvement with respect to the original MAC method and minimizes the error involved in the calculation.

### 3. Code Validation:

The code was validated by simulating the flow over a backward step and the results were compared with the results presented in the literature. Figure 2 presents the streamline plots for the backward facing step case. Figure 2 (a, b, c), present the results obtained from the code developed and the graphs presented in Figure 2 (d, e, f), were obtained by Chowdhary and Dhiman [8]. Three Reynolds numbers of 100, 150 and 200 were studied in both cases. The comparison was in complete agreement in all cases studied, the downstream vortices were steady in all cases and their respective length was the same in all comparisons undertaken.

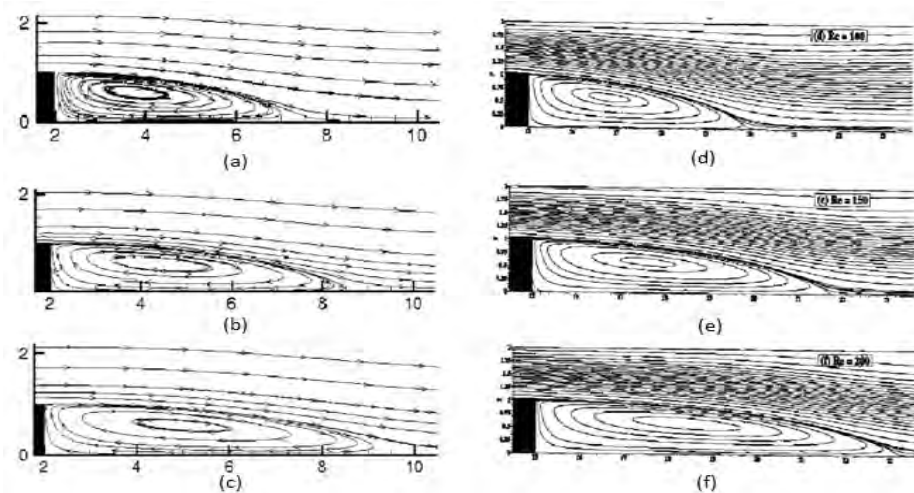


Figure 2: Instantaneous Streamline plots for Reynolds Numbers: (a), (d) Re=100, (b), (e) Re=150 and (c), (f) Re=200. Left hand side figures were generated by the present code, right hand side figures were created by Chowdhary and Dhiman [8].

### 4. Results and Discussion:

From the global flow characteristics, it can be said that the use of ZNMF and FA produce a very similar effect on the downstream wake patterns. Figure 3 presents the equally spaced temporal streamline and vorticity plots in a vortex shedding cycle. It was observed that, at frequency  $f=0.055$ , the vortex shedding was subdued and the drag reduction was found to be maximum. Jet velocity amplitude,  $A$  was 10% of the free stream velocity. It was already observed in previous studies, Creusé et al [4], Dahan et al [1], Hassan [5], among others, that exciting the flow at the vortex shedding natural frequency diminishes downstream vorticity for an appropriate amplitude of the injected jet. Figure 4 presents the vortex shedding when AFC frequency is  $f=0.055$  and the velocity amplitude is  $A=1$ .

For a jet velocity amplitude  $A=0.1$  and the optimum frequency  $f=0.055$ , the drag on the step was minimum, as presented in figure 5b. As the velocity amplitude of the AFC jet increases above 0.1, the drag acting on the body also increases exponentially, figure 5b, and the same trend was observed in both zero net mass flow and fluidic actuator techniques. The increase in drag with jet velocity

amplitude appeared to be higher in the case of fluidic actuators than in the case of zero net mass flow, proving that the technique involving absorption and injection is more effective than just periodic blowing. At high jet velocity amplitudes the energy of the dissipating vortex increases, leading to higher tendency of separation, see figures 4 (a, g) and 4 (d, j). Shear stresses on the upstream surface also increase causing the drag acting on the body to increase exponentially.

On figure 5a, the variation of Drag coefficient with active flow control frequency is presented. It can be observed that for a jet frequency around  $f=0.05$ , the drag coefficient oscillates. The minimum drag values appear at  $f=0.045$  and  $f=0.055$ , which happens to be  $\pm 10\%$  of the natural vortex shedding frequency when no flow control is applied. In the present case  $+10\%$  i.e.  $f=0.055$  is found to be slightly more effective than  $-10\%$  in drag reduction, as seen in figure 5a, hence flow patterns in figures 3 and 4 are presented at this frequency. It is interesting to observe that between the two effective frequencies 0.045 and 0.055 and in both control techniques, the drag seems to increase and decrease following a zigzag cycle. This could be attributed to the resonance effect on the boundary layer in combination of the AFC frequency. Therefore a slight deviation from this frequency leads to instabilities until reaching an effective frequency of  $f=0.05\pm 10\%$ . The frequencies  $f=0.055$  and  $f=0.045$  seem to be the limits of oscillations in the drag coefficient, then the frequencies above and below them, leads to an increase of the drag coefficient.

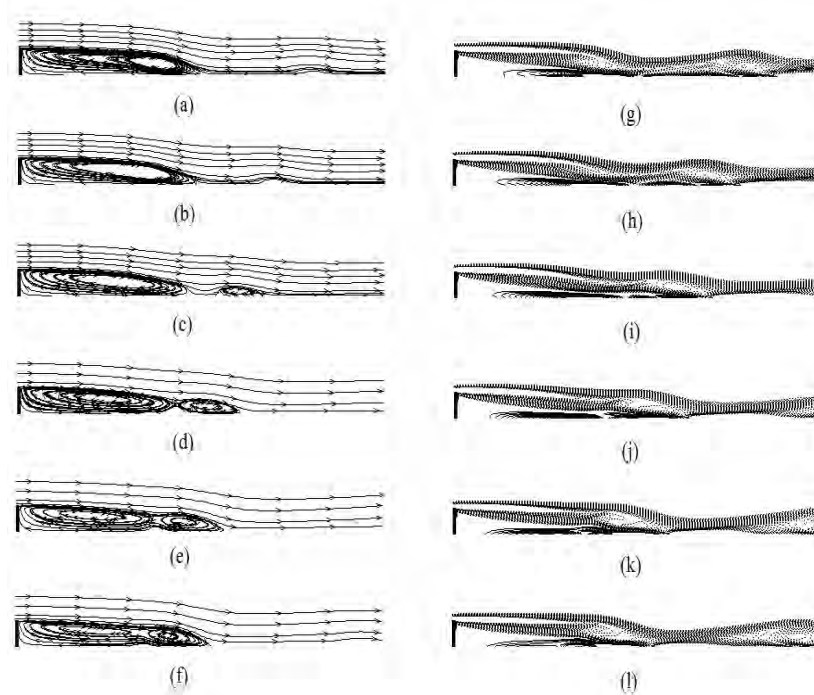


Figure 3: Streamline and corresponding Vorticity plots of vortex shedding cycle in the wake of Backward Step at  $Re=500$ , with upstream zero net mass flow control frequency  $f=0.055$ ,  $A=0.1$  and  $w=0.023a$ . Groove position  $0.047a$ . (a, g)  $T/6$ ; (b, h)  $T/3$ ; (c, i)  $T/2$ ; (d, j)  $2T/3$ ; (e, k)  $5T/6$ ; (f, l)  $T$ .

An interesting phenomena which can be observed from figures 5(a,b) and 6(a,b), is that with the variation of the parameters, the two flow control techniques exhibit similar behavior, although the zero net mass flow technique was found to be more effective than the fluidic actuator technique, regarding drag reduction. In ZNMF actuators, the flow is both absorbed and injected, whereas in FA the flow is only injected, causing a smaller absorption of the dissipating vortex energy in the wake.

Four different groove locations were as well evaluated,  $0.024a$ ,  $0.047a$ ,  $0.072a$  and  $0.097a$ , measured

upstream surface edge. The groove optimum position for both actuating techniques, with respect to maximum drag reduction was 0.047a, as presented in figure 6a. At this position, flow control seems to influence the boundary layer in an efficient manner, to delay the separation and thereby reducing the drag on the body. When the groove is moved further upstream, it leads to boundary layer earlier separation and the drag on the body increases. When the groove is very close to the right edge, the boundary layers seems to become more unstable and separate earlier than in the case of optimum position, thereby enhancing the vortex dissipation and causing the drag to increase, as seen in figure 6a.

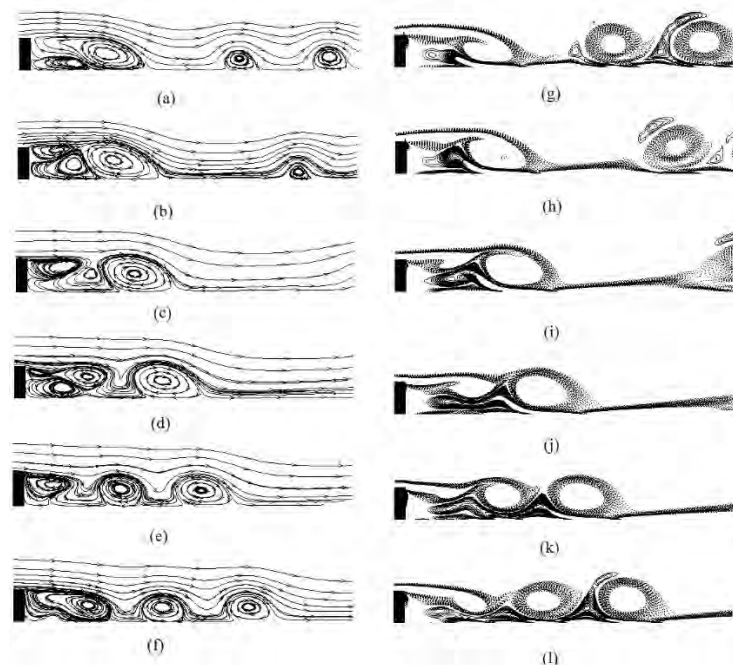


Figure 4: Streamline and corresponding Vorticity plots of vortex shedding cycle in the wake of Backward Step at  $Re=500$ , with upstream zero net mass flow control frequency  $f=0.055$ ,  $A=1$  and  $w=0.023a$ . Groove position 0.047a. (a, g)  $T/6$ ; (b, h)  $T/3$ ; (c, i)  $T/2$ ; (d, j)  $2T/3$ ; (e, k)  $5T/6$ ; (f, l)  $T$ .

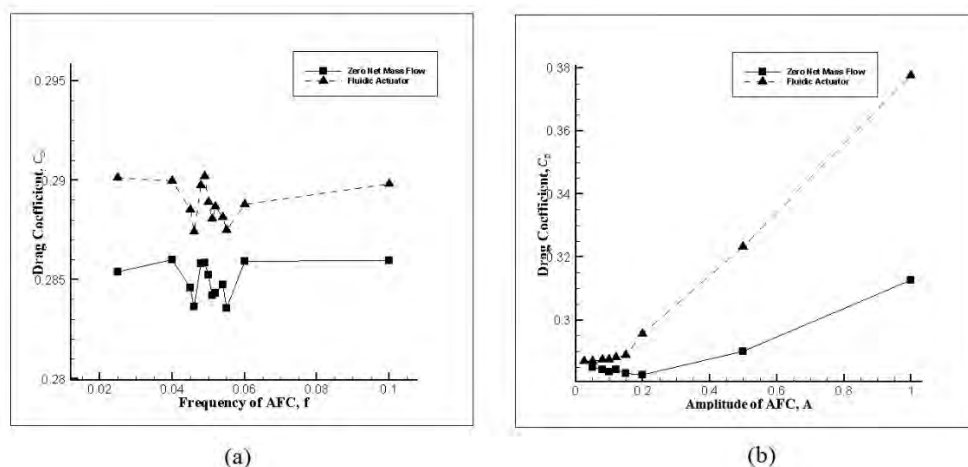


Figure 5: (a) Averaged Drag coefficient versus frequency,  $f$  of active flow control (AFC) (b) Averaged Drag coefficient versus amplitude of AFC,  $A$  at Reynolds number,  $Re=500$ . Groove position 0.047a.

Groove width also plays a very important role regarding the body drag reduction, in the case of fluidic

actuators, the drag acting on the body is directly proportional to the groove width, figure 6b. This is caused due to only injection of the fluid into the boundary layer. As the width increase, the volumetric flow into the boundary layer also increases, leading to more energy being induced into the boundary layer which causes it to separate quickly, increasing the drag acting on the body. In the case of zero net mass flow the drag decreases when the groove width is increased from 0.023a to 0.048a and increases when the width is further increased to 0.074a. The critical width at which the most effective amount of fluid being injected and absorbed into the boundary layer, which reduces the boundary layer instability, is around 5% of the step height. Whereas in the case of fluidic actuators, the most efficient width, was found to be around 2% of the step height, as seen in figure 6b.

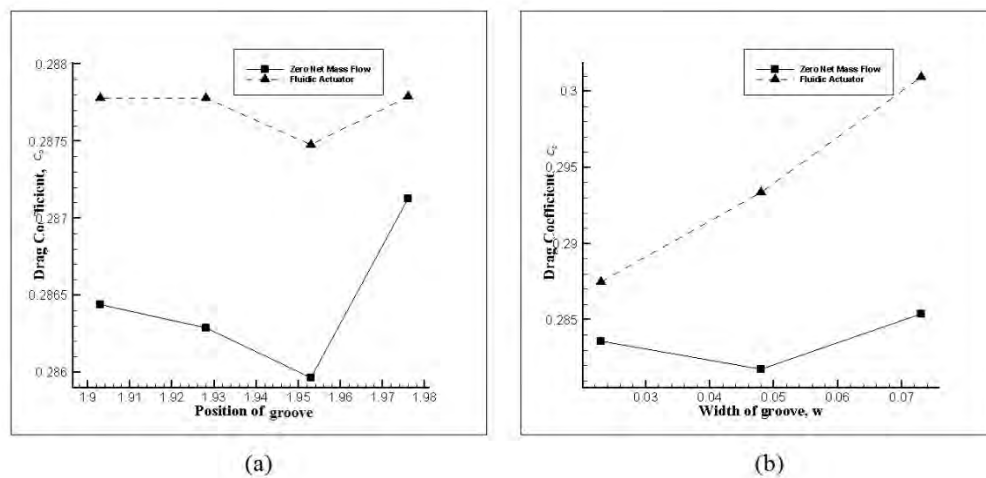


Figure 6: (a) Averaged Drag coefficient versus position of groove (b) Averaged Drag coefficient versus width of the groove,  $w$  at Reynolds number,  $Re=500$

## 5. Conclusions:

- It was found that ZNMF and FA exhibit a similar global behavior.
- The predominant factor affecting the flow is the AFC frequency.
- The optimum frequency was found to be  $\pm 10\%$  of the flow vortex shedding frequency.
- Velocity amplitude of 10% of the upstream velocity was found to be effective in both AFC techniques.
- The most effective position of the groove was 0.047a.
- Optimum groove width for ZNMF was about 5% of the step height, while for FA the optimum groove width was 2% of the step height.

## References

- [1] Dahan Jeremy A., Morgans A.S., Lardeau S. "Feedback control for form-drag reduction on a bluff body with a blunt trailing edge". J. Fluid Mech. 704; 360-387. (2012).
- [2] Dejoan A., Jang Y.-J., Leschziner M.A. "Comparative LES and Unsteady rANS Computations for a Periodically-Perturbed Separated Flow Over a Backward-Facing Step". ASME-Journal of Fluids Engineering. 127; 872-878. (2005).
- [3] Marrot F., Gajan P., Pauzin S., Simon F. "Experimental Application of an Active Control Loop on Backward-Facing Step Flow". AIAA Journal, 43;6; 1176-1186. (2005).
- [4] Creusé E., Giovannini A., Mortazavi I. "Vortex simulation of active control strategies for transitional backward-facing step flows". Computers & Fluids 38; 1348-1360. (2009).
- [5] Hasan M. A. Z. "The flow over a backward-facing step under controlled perturbation: laminar separation". J Fluid Mech. 238; 73-96. (1992).

- [6] Vukasinovic B., Rusak Z., Glezer A. “Dissipative small-scale actuation of turbulent shear layer”. J Fluid Mech. 656; 51-81. (2010).
- [7] Roberts GO. “Computational meshes for boundary layer problems”. Proceedings of the Second International Conference on Numerical Methods and Fluid Dynamics, Lecture Notes in Physics. Springer-Verlag: New York. 8;171–177. (1971).
- [8] Chowdhary H., Dhiman A. Two-Dimensional Laminar Fluid Flow and Heat Transfer over a Backward-Facing Step: Effects of Reynolds and Prandtl Numbers. Heat transfer research journal. 42: 4; 379-402 (2011).